UM-TH-99-02
hep-ph/9903468
Spring Equinox, 1999

WIMP Velocity Impact on Direct Dark Matter Searches

Michal Brhlik[a] and Leszek Roszkowski[b]

[a] *Randall Physics Lab*
University of Michigan
Ann Arbor, MI 48109-1120, USA

[b] *Department of Physics*
Lancaster University
Lancaster LA1 4YB, UK

Abstract

We examine the effect of some uncertainties in the input astrophysical parameters on direct detection searches for WIMPs in the Galactic halo. We concentrate on the possible WIMP annual modulation signal recently reported by the DAMA Collaboration. We find that allowing for a reasonable uncertainty in a WIMP Maxwellian velocity distribution leads to significantly relaxed constraints on the WIMP mass as compared to the original DAMA analysis.

1 Introduction

It is generally assumed that spiral galaxies are surrounded by extended halos of dark matter (DM) for which a likely candidate is a hypothetical stable and neutral particle generically called a weakly interacting massive particle (WIMP). Experimental sensitivity has now improved to the level at which a signal from well-motivated WIMP candidates, like the neutralino of supersymmetry (SUSY), could be detected [1]. However, inherent astrophysical and other uncertainties are likely to considerably weaken experimental limits and regions of a possible WIMP signal.

One of the most promising ways to look for WIMPs in the halo of the Milky Way is the one based on annual modulation [2, 3]. A WIMP signal rate depends on the effective velocity of an incident WIMP on a detector target which in turn depends on the Earth's velocity v_e in the Galactic frame and on the WIMP velocity distribution in the halo. The Earth's motion in the Galactic frame is a superposition of its rotation around the Sun with that of the Sun around the Galactic center,

$$v_e(t) = v_\odot + v_\otimes \cos\gamma \cos\left(\frac{2\pi(t-t_p)}{T}\right) \tag{1}$$

where $v_\odot \approx 232\,\mathrm{km/s}$ and $v_\otimes \approx 30\,\mathrm{km/s}$ are the respective rotational velocities of the Sun and the Earth, $\gamma = 60^\circ$ is the angle between the two planes of rotation, $T = 1\,\mathrm{yr}$ and the peak occurs on $t_p = 153\,\mathrm{rd}$ day of the year (around the 2nd of June). Although the effect is expected to be small, around a few per cent, with enough sensitivity it is measurable.

The annual modulation method has been adopted by the DAMA Collaboration in a Gran Sasso Laboratory-based experiment involving a detector consisting of nine 9.70 kg NaI(Tl) crystals. Based on the statistics of $14,962\,\mathrm{kg}\times\mathrm{day}$ of data collected over a period from November '96 to July '97 (part of run II), the Collaboration has recently reported [4] a statistically significant effect which could be caused by an annual modulation signal due to a WIMP with mass m_χ and WIMP-proton cross section σ_p given as

$$m_\chi = 59\,\mathrm{GeV}^{+17}_{-14}\,\mathrm{GeV} \qquad \xi\sigma_p = 7.0^{+0.4}_{-1.2}\times 10^{-6}\,\mathrm{pb} \quad \text{(at 99.6\% CL)}, \tag{2}$$

where $\xi = \rho_\chi/\rho_{0.3}$ stands for the local WIMP mass density ρ_χ normalized to $\rho_{0.3} = 0.3\,\mathrm{GeV/cm^3}$. (See also Figure 6 in Ref. [4] for a 2σ signal region in the $(m_\chi, \xi\sigma_p)$ plane.) According to DAMA, the new analysis is consistent with and confirms the Collaboration's earlier hint [5] for the presence of the signal based on $4,549\,\mathrm{kg}\times\mathrm{day}$ of data.

In this Letter, we point out that the region selected by DAMA as corresponding to a possible WIMP signal strongly depends on the assumed values of astrophysical parameters which are poorly known. Given the fact that the Galactic halo has not been directly observed, nor any of its parameters have been actually measured, we advocate a more conservative approach. We demonstrate the effect by varying the position of

the peak of the WIMP velocity distribution which, following DAMA and a standard lore, we assume here to be Maxwellian. We find that significantly larger ranges of especially WIMP mass and, to a lesser extent, $\xi\sigma_p$ should be considered as consistent with the possible annual modulation effect reported by DAMA. This will have important implications for the allowed configurations of SUSY masses and couplings.

In Section 2 we summarize the relevant elements of the DAMA analysis. In Section 3 we present the method which we use for calculating the expected event rate from Majorana WIMPs in annual modulation. Results and conclusions are presented in Section 4.

2 DAMA Analysis

The expected WIMP signal event rate (see Section 3 for details) is proportional to the elastic WIMP-nucleus cross section $\sigma(\chi N)$, the local WIMP number density ρ_χ/m_χ and the density of the target nuclei with mass m_A. The local WIMP density enters multiplicatively and it is possible to account for its variation by normalizing it to some nominal value, *e.g.*, $\rho_{0.3}$ in Ref. [4], and multiplying the scattering cross section by ξ. The event rate also depends on the velocity of a halo WIMP relative to the detector but this dependence is highly non-trivial and cannot be factorized out.

Assuming the WIMP velocity distribution to be characterized by a parameter v_0, one can re-write Eq. (1) as

$$\eta(t) = \eta_0 + \Delta\eta \cos\left(\frac{2\pi(t-t_p)}{T}\right) \tag{3}$$

where $\eta = v_e/v_0$, $\eta_0 = v_\odot/v_0$, and $\Delta\eta = v_\otimes \cos\gamma/v_0$. Since $v_\odot \gg v_\otimes$ and it is expected that $v_0 \sim v_\odot$, it is reasonable to assume that $\eta_0 \gg \Delta\eta$. This was used by DAMA to approximate the differential signal event rate in the k-th energy bin by the first two terms in Taylor's expansion [5]

$$\begin{aligned} S_k\left[\eta(t)\right] &= S_k\left[\eta_0\right] + \left[\frac{\partial S_k}{\partial\eta}\right]_{\eta_0} \Delta\eta \cos\left(\frac{2\pi(t-t_p)}{T}\right) \\ &= S_{0,k} + S_{m,k}\cos\left(\frac{2\pi(t-t_p)}{T}\right). \end{aligned} \tag{4}$$

Using a maximum likelihood method [4, 5], the (time-independent) background was separated from the constant component $S_{0,k}$ and the time-dependent component $S_{m,k}$. Because of the difference in the profiles of the expected energy distributions, the largest contribution to the signal was expected from the lowest energy bins above the threshold [5].

Based on the statistics of $14,962\,\mathrm{kg}\times\mathrm{day}$ of data, values of $S_{0,k}$ and $S_{m,k}$ were obtained between 2 keV (the software threshold) and 20 keV as shown in the Table [4].

Energy (keV)	$S_{0,k} \pm \sigma_{0,k}$ (cpd/kg/keV)	$S_{m,k} \pm \sigma_{m,k}$ (cpd/kg/keV)
2 - 3	0.54 ± 0.15	0.018 ± 0.009
3 - 4	0.23 ± 0.08	0.012 ± 0.004
4 - 5	0.09 ± 0.04	0.006 ± 0.002
5 - 6	0.04 ± 0.02	0.003 ± 0.001

Above 6 keV the detected time-dependent component is statistically insignificant.

As mentioned above, it is possible to write $S_{0,k} = \xi\sigma_p S'_{0,k}$ and $S_{m,k} = \xi\sigma_p S'_{m,k}$ [5]. Both $S'_{0,k}$ and $S'_{m,k}$ depend on WIMP mass but also on its velocity distribution, in addition to several other detector and nuclear factors. Expressions for $S'_{0,k}$ and $S'_{m,k}$ used by DAMA can be found in Ref. [6]. The ranges (2) of m_χ and $\xi\sigma_p$ in agreement with the hypothesis of an annual modulation signal due to a Majorana WIMP with dominant spin independent interaction with NaI target were obtained by a maximum likelihood method [4]. The period was assumed to be one year and the position of the peak was fixed at the expected value.

We note that in DAMA's analysis a spherical halo model and a Maxwellian velocity distribution with a *fixed* value of $v_0 = \sqrt{2/3}v_{\rm rms} = 220\,{\rm km/s}$ was assumed [4]. We will argue that the ranges of m_χ and $\xi\sigma_p$ depend sensitively on the assumed value of v_0. First we will present the procedure which we use.

3 Majorana WIMP Detection Rate in NaI Detectors

Elastic interactions of relic WIMPs with nuclei in the detector result in a nuclear recoil energy deposit in the detector volume. Their size depends on the cross section of the WIMP scattering off constituent quarks and gluons. For non-relativistic Majorana particles, these can be divided into two separate types [7]. The coherent part described by an effective scalar coupling between the WIMP and the nucleus is proportional to the number of nucleons in the nucleus. It receives a tree-level contribution from scattering off quarks, $\chi q \to \chi q$, as described by a Lagrangian $\mathcal{L} \sim (\chi\chi)\,(\bar{q}q)$. The incoherent component of the WIMP-nucleus cross section results from an axial current interaction of a WIMP with constituent quarks, given by $\mathcal{L} \sim (\chi\gamma^\mu\gamma_5\chi)\,(\bar{q}\gamma_\mu\gamma_5 q)$, and couples the spin of the WIMP to the total spin of the nucleus.

In the case of a supersymmetric neutralino, there are several diagrams contributing to the scalar part, mainly from Higgs exchange and squark exchange with, in general, non-degenerate left and right squark soft masses. Another contribution to coherent interactions comes from one-loop neutralino-gluon scattering where the exchanged Higgs couples to a heavy quark loop on a gluon line [8]. The axial interaction is due to the Z and squark exchange.

The differential cross section for a WIMP scattering off a nucleus X^A_Z with mass m_A

is therefore expressed as

$$\frac{d\sigma}{d|\vec{q}|^2} = \frac{d\sigma^{scalar}}{d|\vec{q}|^2} + \frac{d\sigma^{axial}}{d|\vec{q}|^2}, \tag{5}$$

where the transferred momentum $\vec{q} = \frac{m_A m_\chi}{m_A + m_\chi}\vec{v}$ depends on the velocity $\vec{v}$ of the incident WIMP. The effective WIMP-nucleon cross sections σ^{scalar} and σ^{axial} are computed by evaluating nucleonic matrix elements of corresponding WIMP-quark and WIMP-gluon interaction operators.

In the scalar part contributions from individual nucleons in the nucleus add coherently and the finite size effects are accounted for by including the scalar nuclear form factor $F(q)$. (The effective interaction in general also includes tensor components but the relevant nucleonic matrix elements can be expanded in the low momentum-transfer limit in terms of the nucleon four-momentum and the quark (gluon) parton distribution function. As a result, the non-relativistic WIMP-nucleon Lagrangian contains only scalar interaction terms.) The differential cross section for the scalar part then takes the form [1]

$$\frac{d\sigma^{scalar}}{d|\vec{q}|^2} = \frac{1}{\pi v^2}[Z f_p + (A - Z) f_n]^2 F^2(q), \tag{6}$$

where f_p and f_n are the effective neutralino couplings to protons and neutrons, respectively. Explicit expressions for the case of the supersymmetric neutralino can be found in the Appendix of Ref. [9].

The effective axial WIMP coupling to the nucleus depends on the spin content of the nucleon $\Delta q_{p,n}$ and the overall expectation value of the nucleon group spin in the nucleus $< S_{p,n} >$. For a nucleus with a total angular momentum J we have

$$\frac{d\sigma^{axial}}{d|\vec{q}|^2} = \frac{8}{\pi v^2}\Lambda^2 J(J+1) S(q), \tag{7}$$

with $\Lambda = \frac{1}{J}[a_p \langle S_p \rangle + a_n \langle S_n \rangle]$. The axial couplings

$$a_p = \frac{1}{\sqrt{2}} \sum_{u,d,s} d_q \Delta q^{(p)}, \qquad a_n = \frac{1}{\sqrt{2}} \sum_{u,d,s} d_q \Delta q^{(n)} \tag{8}$$

are determined by the experimental values of the spin constants $\Delta u^{(p)} = \Delta d^{(n)} = 0.78$, $\Delta d^{(p)} = \Delta u^{(n)} = -0.5$ and $\Delta s^{(p)} = \Delta s^{(n)} = -0.16$. The effective couplings d_q depend on the WIMP properties and for the neutralino they can be found in the Appendix of Ref. [9].

In translating $\sigma(\chi q)$ and $\sigma(\chi g)$ into the WIMP-nucleon cross section in Eq. (5) several uncertainties arise. The nucleonic matrix element coefficients for the scalar interaction are not precisely known. Also, the spin content of the nucleon and the expectation values of the proton (neutron) group spin in a particular nucleus are fraught with significant uncertainty and nuclear model dependence. These ambiguities have to

be considered in numerical calculations. Finally, in order to obtain $\sigma(\chi N)$, models of nuclear wave functions must be used. The scalar nuclear form factor reflects the mass density density distribution in the nucleus. Following DAMA analysis we take the form factor for Na to be equal to one while for I we use the Saxon-Woods form factor [10]

$$F(q) = \frac{3j_1(qR_0)}{qR_1} e^{-\frac{1}{2}(qs)^2}, \tag{9}$$

where $R_1 = \sqrt{R^2 - 5s^2}$, $R = A^{\frac{1}{3}} \times 1.2\,\mathrm{fm}$, j_1 is a spherical Bessel function and $s = 1\,\mathrm{fm}$.

The spin form factor for I is assumed to be

$$S(q) = [0.6845e^{-359.1q^2} - 3.427q^2 + 0.3042]e^{-0.2q^2(r_I^2 - r_{Xe}^2)} \tag{10}$$

where q is in GeV and the nuclear radius is $r = 1.2A^{1/3}\,\mathrm{fm}$. The finite size effects for Na can be neglected. The nucleon group spin expectation values for I have been estimated within the quenched interacting boson model giving $< S_p >= 0.128$ and $< S_n >= 0$ [11], and for Na we use the odd group model result $< S_p >= 0.136$ and $< S_n >= 0$ [12].

In order to calculate the WIMP detection rate for a given material, it is necessary to convolute the cross section Eq. (5) with the local WIMP flux which, in the rest frame of the detector, will be time-dependent. The differential event rate can be expressed as [1]

$$\begin{aligned} \frac{dR}{dE_R} &= \frac{4}{\sqrt{\pi^3}} \frac{\rho_\chi}{m_\chi} \widetilde{T}(E_R) \Big\{ [Zf_p + (A - Z)f_n]^2 F^2(q) \\ &\quad + 8\Lambda^2 J(J+1) S(q) \Big\}, \end{aligned} \tag{11}$$

where $E_R = \frac{|\vec{q}|^2}{2m_A}$ is the recoil energy of the nucleus. The time-dependent function $\widetilde{T}(E_R)$ integrates over all possible kinematic configurations in the scattering process

$$\widetilde{T}(E_R) = \frac{\sqrt{\pi}}{2} \int_{v_{min}}^{\infty} \frac{f_\chi}{v}\, dv. \tag{12}$$

For a Maxwellian velocity distribution taking into account the motion of the Sun and the Earth, Eq. (1), one obtains

$$\widetilde{T}(E_R) = \frac{\sqrt{\pi}}{4v_e} \left[Erf\left(\frac{v_{min} + v_e(t)}{v_0} \right) - Erf\left(\frac{v_{min} - v_e(t)}{v_0} \right) \right], \tag{13}$$

with $v_{min} = \sqrt{\frac{E_R(m_\chi + m_A)^2}{2m_\chi^2 m_A}}$.

The actually measured response from a nucleus X hit by a WIMP is only a fraction of the recoil energy, $E = q_X E_R$. It is also called the electron equivalent energy and is determined by the quenching factor q_X which is different for each detector material. Here we assume numerical values of the quenching factors $q_{Na} = 0.30$ and $q_I = 0.09$ as they were reported by the DAMA Collaboration [6] in agreement with previously published results [13].

The expected experimental spectrum per energy bin can then be expressed as

$$\frac{\Delta R}{\Delta E}(E) = r_{Na} \int_{E/q_{Na}}^{(E+\Delta E)/q_{Na}} \frac{dR_{Na}}{dE_R}(E_R)\,\frac{dE_R}{\Delta E} + r_I \int_{E/q_I}^{(E+\Delta E)/q_I} \frac{dR_I}{dE_R}(E_R)\,\frac{dE_R}{\Delta E}, \qquad (14)$$

where $r_{Na} = \frac{M_{Na}}{M_{Na}+M_I} = 0.153$ and $r_I = \frac{M_I}{M_{Na}+M_I} = 0.847$ are the respective mass fractions of Na and I in the detector material.

The formulae presented here are in full agreement with those used by DAMA [6]. The fact that we neglect the WIMP escape velocity from the halo (estimated in Ref. [2] between 580 km/s and 625 km/s) leads to a negligible numerical difference. The differential event rate in Eq. (11) is dominated by the scalar contribution due to WIMP scattering off iodine. In our calculation we assume that $f_p \approx f_n$ [1] and use f_p as a free parameter which can be directly translated into the WIMP cross section on proton $\sigma_p = \frac{4m_p^2 m_\chi^2}{\pi(m_p+m_\chi)^2} f_p^2$. In this approximation one can re-write Eq. (11) as

$$\frac{dR}{dE_R} = (\xi\sigma_p)\left[\frac{\rho_{0.3}}{\sqrt{\pi}}\frac{(m_p+m_\chi)^2}{m_p^2 m_\chi^3} A^2 \widetilde{T}(E_R) F^2(q).\right] \qquad (15)$$

Theoretical prediction for the signal is then calculated using Eqs. (11) and (14) with $\Delta E = 1$ keV. The predicted rates in each channel are evaluated for $t = t_p$ and $t = t_p + T/2$, and Eq. (4) is used to extract the predicted values $S_{0,k}^{th}$ and $S_{m,k}^{th}$. These are compared with the experimental values given in the Table, as described below.

4 Results and Conclusions

Our goal is to examine how the sensitivity of the expected event spectrum will depend on the velocities of incident WIMPs. It is clear that these enter in a rather complicated way, through Eq. (13), but also through the transferred momentum q on which the form factors depend.

Experimental determinations of the Galactic halo velocity distributions are rather uncertain. Assuming a spherically symmetric and isotropic halo with a Maxwellian dark matter velocity distribution, it was argued in Ref. [2] that v_0 should be of order of the local Galactic rotation velocity. Several values have been reported for the latter: 243 ± 20 km/s [14], 222 ± 20 km/s [15], 228 ± 19 km/s [16], although a much larger spread 220 ± 57 km/s was also recently quoted [17]. To be consistent with the DAMA analysis where a fixed value of $v_0 = 220$ km/s was assumed, we take $v_0 = 220 \pm 20$ km/s.

We first illustrate in Figure 1 the effect of the dependence of the expected event spectrum on the velocities of incident WIMP. We plot the expected differential event rate versus the detected energy E for several choices of v_0. We find a significant dependence on v_0 at both smaller and larger values of the detected energy. The effect is caused by the dependence of $\widetilde{T}$ on the position of the peak of the WIMP velocity distribution v_0. At fixed m_χ and σ_p, $\widetilde{T}(E)$ increases with v_0 for both sodium and iodine.

The bending appearing in the spectra at lower values of $\frac{\Delta R}{\Delta E}$ is caused by the contribution from WIMPs scattering off Na nuclei becoming larger than that off iodine.

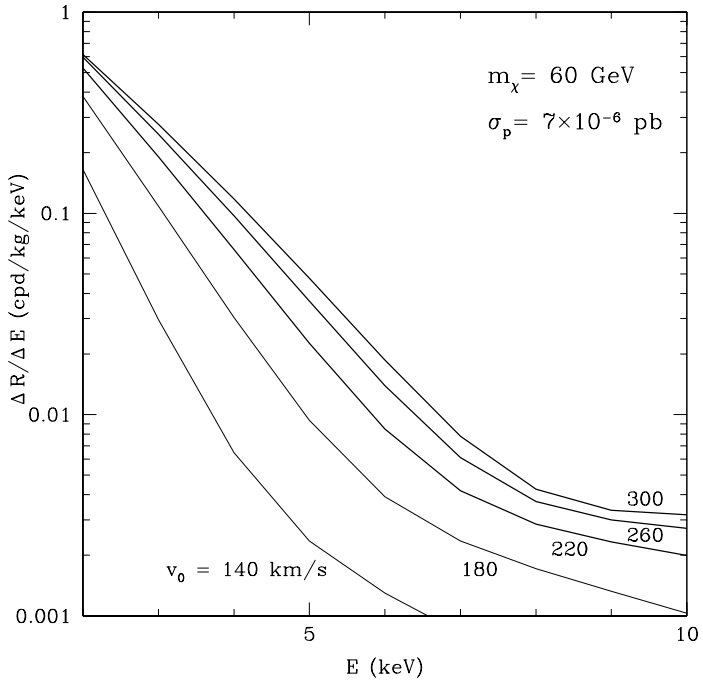

Figure 1: The expected differential event rate spectrum versus the detected energy E for $m_\chi = 60\,\mathrm{GeV}$, $\sigma_p = 7 \times 10^{-6}\,\mathrm{pb}$ and several choices of v_0.

The latter decreases more rapidly with energy due to a smaller quenching factor. It is worth noting that in the future, with large enough statistics available, the position of the bending, which depends on the WIMP's mass and velocity, could provide additional information about the signal.

In order to compare the experimental spectrum measured by DAMA with theoretical WIMP predictions, we introduce a function κ defined as

$$\kappa = \sum_k \frac{\left(S_{0,k}^{th} - S_{0,k}^{exp}\right)^2}{\sigma_{0,k}^2} + \sum_k \frac{\left(S_{m,k}^{th} - S_{m,k}^{exp}\right)^2}{\sigma_{m,k}^2} \tag{16}$$

with the experimental errors of both the time-independent and time-dependent signal components $\sigma_{0,k}$ and $\sigma_{m,k}$, respectively, serving as weights. (They are defined in the Table.) Minimization of this function is then used to look for the ranges of WIMP masses and cross sections which would best fit the ranges of $S_{0,k}$ and $S_{m,k}$ responsible for DAMA's possible annual modulation signal.

We stress that the function κ cannot serve as a substitute for a dedicated maximum likelihood analysis employed by DAMA where detector efficiencies for each crystal and other factors were included to evaluate the background and both the signal components $S_{0,k}$ and $S_{m,k}$. Only a full experimental analysis can lead to selecting a region in the plane $(m_\chi, \xi\sigma_p)$ consistent with the signal. Nevertheless, we believe that κ is an adequate tool

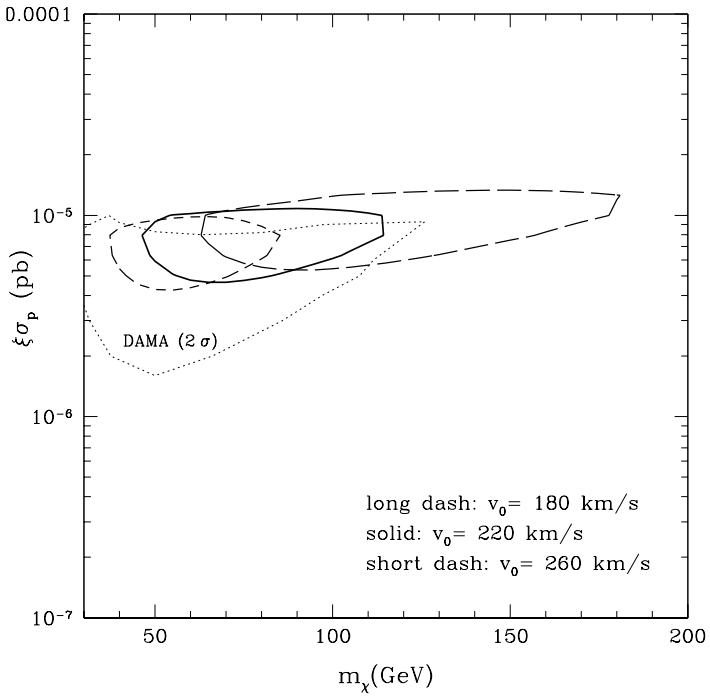

Figure 2: Contours of the function $\kappa = 10$ (Eq. 16) for different values of the peak of the halo WIMP Maxwellian velocity distribution. Denoted by dots is the 2σ region selected by DAMA assuming $v_0 = 220\,\mathrm{km/s}$.

to demonstrate the dependence of a signal region on WIMP velocities. This is presented in Figure 2 where we plot contours of $\kappa = 10$ for $v_0 = 220\,\mathrm{km/s}$ (solid), which is the value used by DAMA, and for $v_0 = 180\,\mathrm{km/s}$ (long dash) and $v_0 = 260\,\mathrm{km/s}$ (short dash) corresponding to a 2σ error in v_0. We note that the function κ is well-focused and that the contour $\kappa = 10$ reproduces the 2σ region of DAMA (the dotted curve in Figure 2 adopted from Figure 6 in Ref. [4]) remarkably well. Any other choice of κ below 20 or so would give only somewhat more relaxed contours.

The region of $\kappa = 10$ slides quickly to the right and becomes much more elongated for v_0 decreasing from the value $v_0 = 220\,\mathrm{km/s}$ used in the DAMA analysis [4]. We find a significant relaxation of the upper limit on m_χ even for values of v_0 much closer to $v_0 = 220\,\mathrm{km/s}$. For example, for $v_0 = 200\,\mathrm{km/s}$, the region reaches $m_\chi \approx 140\,\mathrm{GeV}$. For v_0 larger than $220\,\mathrm{km/s}$ the region moves to the left and becomes much more confined. Its vertical position decreases only very slowly with increasing velocity.

It is clear from Figure 2 that the dependence of κ on v_0 is very strong and cannot be neglected. This effect is particularly important for smaller WIMP velocities as it allows for substantially larger values of the WIMP mass to be considered compatible with the possible annual modulation signal from DAMA, as already emphasized in Ref. [18]. (A crude estimate of the effect was also given in Ref. [19].) We find that varying v_0 within

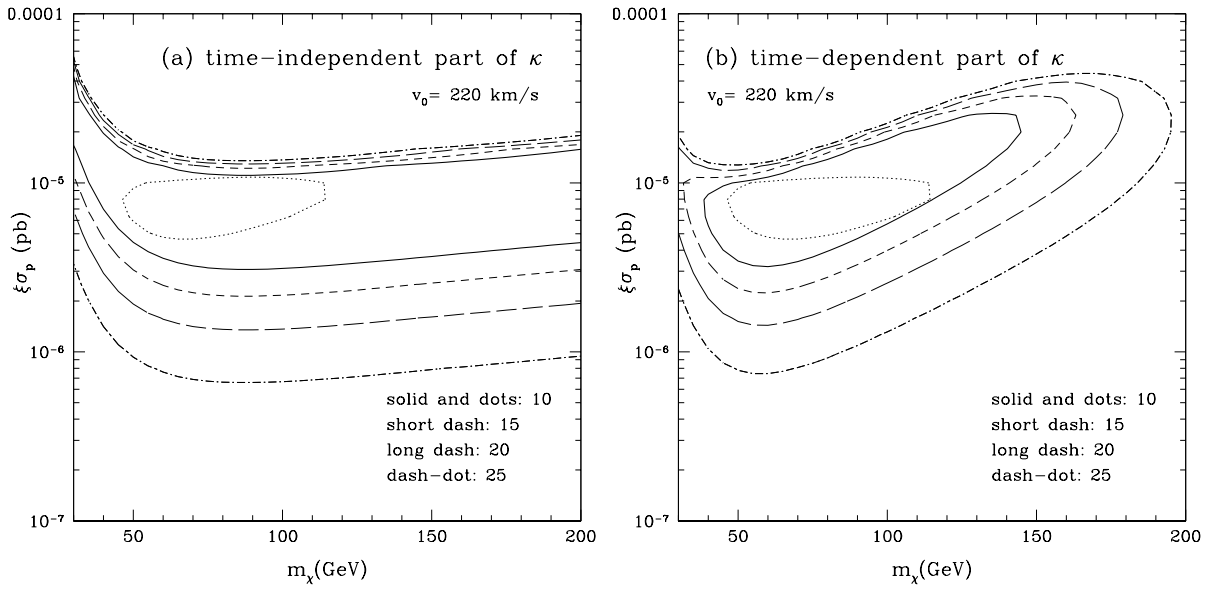

Figure 3: Several contours of (a) the time-independent and (b) time-dependent parts of κ for $v_0 = 220\,\mathrm{km/s}$. Denoted by dots is the contour of 10 of total κ.

the 2σ range around $220\,\mathrm{km/s}$ ($180 \lesssim v_0 \lesssim 260\,\mathrm{km/s}$) leads to increasing the upper limit for m_χ by nearly 60% while on the lower side of m_χ the relaxation is only about 25%. The range of the $\xi\sigma_p$ values increases by about 10%.

Next we examine the relative contributions from the time-independent and time-dependent parts to the shape of κ contours. This is shown in Figure 3 for the case $v_0 = 220\,\mathrm{km/s}$. We find an interesting interplay. The time-independent part of κ quickly increases around $1.1 \times 10^{-5}\,\mathrm{pb}$ (except for smaller $m_\chi \lesssim 50\,\mathrm{GeV}$) but does not put any restriction on large m_χ. It is the time-dependent part which cuts off the large WIMP mass region allowed by the constant component while at the same time favoring larger values of $\xi\sigma_p$ at larger m_χ. With more data taken over a full period or more available, this property may allow one to derive a stronger upper bound on m_χ, despite large uncertainties in halo WIMP velocities.

In this Letter, we emphasized the importance of astrophysical uncertainties in determining the shape and overall position of the expected detection spectrum. We did this by demonstrating how varying the maximum of the Maxwellian velocity distribution of Galactic halo WIMPs will considerably relax the region selected by DAMA as corresponding to a possible annual modulation signal. (It is our understanding that the DAMA Collaboration is currently in the process of incorporating the effect in their annual modulation analysis [20].) The effect will also affect WIMP exclusion plots which are often drawn for one fixed value of v_0, and should be of interest to those involved in searches for halo WIMPs.

Clearly, there are several other uncertainties entering the halo WIMP detection analysis. We reiterate that, while there is much convincing astrophysical evidence for the existence of the Galactic halo, parameters describing its shape have only been established through indirect methods and their values should be considered as rather uncertain. There still remains a considerable spread among possible models for the Galactic halo and (halo model dependent) quoted error bars for v_0, and the local halo density should, in our opinion, be taken with extreme caution. (In Ref. [17] several halo models were compared with the standard non-rotating spherical model and their effect on the direct rates was found to be minimal.) Nuclear physics uncertainties in the form factors are also rather poorly known and have been of much concern [21].

We conclude that, due to astrophysical input uncertainties, caution should be taken when considering exclusion regions from detection experiments and also in analyzing their implications on underlying WIMP models. For example, it has been claimed [22, 23] that, in supersymmetric models with the lightest neutralino as the stable superpartner and a WIMP candidate, it is possible to find SUSY configurations consistent with the possible annual modulation signal of DAMA but only for large enough $\tan\beta \gtrsim 10$, typically rather small relic abundance, and for restricted ranges of other SUSY parameters. Including the effect of astrophysical uncertainties will lead to much broader ranges of allowed parameters than previously thought [24].

Acknowledgements

One of us (LR) is grateful to R. Bernabei for a number of clarifying discussions about DAMA's analysis and to T. Sloan for helpful remarks on the manuscript.

References

[1] G. Jungman, M. Kamionkowski and K. Griest, Phys. Rep. **267**, 195 (1996).

[2] A. Drukier, *et al.*, Phys. Rev. **D33**, 3495 (1986).

[3] K. Freese, *et al.*, Phys. Rev. **D37**, 3388 (1988).

[4] R. Bernabei, *et al.*, University of Rome preprint ROM2F/98/34 (27 August 1998).

[5] R. Bernabei, *et al.*, Phys. Lett. **B424**, 195 (1998).

[6] R. Bernabei, *et al.*, Phys. Lett. **B389**, 757 (1996).

[7] M. Goodman and E. Witten, Phys. Rev. **D31**, 3059 (1985).

[8] M. Drees and M. Nojiri, Phys. Rev. **D47**, 4226 (1993) and Phys. Rev. **D48**, 3483 (1993).

[9] H. Baer and M. Brhlik, Phys. Rev. **D57**, 567 (1998).

[10] J. Engel, Phys. Lett. **B264**, 114 (1991).

[11] F. Iachello, L.M. Krauss and G. Maino, Phys. Lett. **B254**, 220 (1991).

[12] R. Flores and J. Ellis, Nucl. Phys. **B400**, 25 (1993).

[13] K. Fushimi, *et al.*, Phys. Rev. **C47** (1993) R425; P.F. Smith, *et al.*, Phys. Lett. **B379**, 299 (1996); G.J. Davies, *et al.*, Phys. Lett. **B322**, 159 (1994).

[14] G.R. Knapp, S.D. Tremaine, and J.E. Gunn, Astron. J. **83** (1978) 1585.

[15] F.J. Kerr and D. Lynden-Bell, Mon. Not. R. Astr. Soc. **221** (1986) 1023.

[16] J.A.R. Caldwell and J.M. Coulson, Astron. J. **93** (1987) 1090.

[17] M. Kamionkowski and A. Kinkhabwala, Phys. Rev. **D57**, 3256 (1998).

[18] L. Roszkowski, talk at COSMO-98, Asilomar, USA, November '98, hep-ph/9903467.

[19] N. Fornengo, talk at IDM-98, Buxton, UK, September '98, hep-ph/9812210.

[20] A. Bottino and R. Bernabei, private communication.

[21] See, *e.g.*, Ref. [1] or N.J.C. Spooner, Proc. Int. Workshop on Particle Physics and Cosmology (COSMO-97), World Scientific, Ed. L. Roszkowski.

[22] A. Bottino, F. Donato, N. Fornengo, and S. Scopel, hep-ph/9808456, hep-ph/9808459, and hep-ph/9809239.

[23] R. Arnowitt and P. Nath, hep-ph/9902237.

[24] M. Brhlik and L. Roszkowski, in preparation.